Graphene Surface-Anchored Fluorescence Sensor for Sensitive Detection of MicroRNA Coupled with Enzyme-Free Signal Amplification of Hybridization Chain Reaction

Lang Yang, Chenghui Liu,* Wei Ren, and Zhengping Li*

Key Laboratory of Medicinal Chemistry and Molecular Diagnosis, Ministry of Education; College of Chemistry and Environmental Science, Hebei University, Baoding 071002, Hebei Province, P. R. China

Ⓢ Supporting Information

ABSTRACT: A new enzyme-free signal amplification-based assay for microRNA (miRNA) detection is developed by using hybridization chain reaction (HCR) coupled with a graphene oxide (GO) surface-anchored fluorescence signal readout pathway. MiRNAs can efficiently initiate HCR between two species of fluorescent hairpin probes. After HCR, both of the excess hairpin probes and the HCR products will be anchored on the GO surface. The fluorescence of the hairpin probes can be completely quenched by GO, whereas the HCR products maintain strong fluorescence. Therefore, integrating HCR strategy for signal amplification with selective fluorescence quenching effects of GO provides a versatile miRNA assay.

KEYWORDS: graphene oxide, hybridization chain reaction, MicroRNA, fluorescence sensor, enzyme-free, fluorescence imaging
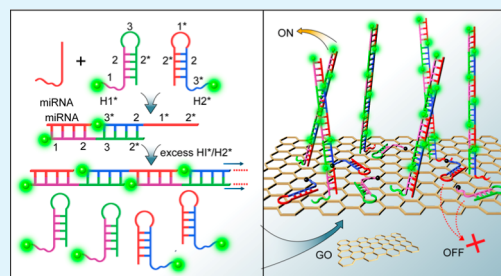
1. INTRODUCTION

MicroRNAs (miRNAs) play key roles in gene expression regulation[1,2] and the development of many types of cancers or diseases is closely related to the abnormal expression of certain miRNAs.[3] Therefore, the sensitive detection of specific miRNAs is of great significance for further understanding of miRNAs' functions as well as clinical diagnosis.[4]

Since many important miRNAs of interest are in quite low abundance in biological samples,[5,6] some nucleic acid amplification techniques are generally required to achieve high sensitivity for miRNA detection, such as RT-PCR,[7,8] ligase chain reaction,[9] ribozyme amplification,[10] the modified invader assay,[11] and some isothermal amplification techniques.[12−14] However, these methods are highly enzyme-dependent, in which one or more types of enzymes are indispensable to catalyze the amplification reactions. Therefore, the reaction conditions such as pH, temperature and buffer media must be precisely controlled in order to guarantee the activity of the enzymes. More importantly, because the enzyme activity is prone to be affected by the environmental media, these enzyme-based amplification assays require relatively clean samples for miRNA detection, which greatly limits their applications in complicated biological samples especially for in situ analysis of miRNAs in living cells.

In this regards, enzyme-free amplification methods have shown great potential in nucleic acid detection.[15−20] Among these enzyme-free approaches, hybridization chain reaction (HCR) is one of the most attractive.[15−17] In HCR, two species of DNA hairpin probes that can coexist stably in solution are rationally designed. However, the introduction of a nucleic acid target can initiate a cascade of hybridization events between the two species of metastable hairpin probes to "polymerize" into a nicked double-stranded DNA (dsDNA) structure. The most attractive advantages of HCR are that it is a kinetics-controlled reaction and the amplification does not require any enzymes. Therefore, HCR has been shown to be an ideal choice for nucleic acid amplification especially in complex biosamples.[21,22] However, the HCR is generally initiated by single and short DNA strands, which seriously limits its application for genomic DNA analysis.

Herein, we report for the first time that small miRNAs are well-suited to efficiently initiate HCR and subsequently, graphene oxide (GO) can be used to completely quench the fluorescence of single fluorophore-labeled hairpin probes. Meanwhile, the HCR products can maintain strong fluorescence. The GO-assisted HCR method, therefore, provides a simple and sensitive approach for miRNA detection in a homogeneous solution. Most importantly, it is found that the HCR products are anchored on the surface of GO. Consequently, GO can be used as the carrier to accumulate the HCR products and enrich the fluorescence signal in a fixed area, which is greatly significant for in situ fluorescence imaging analysis of miRNAs.
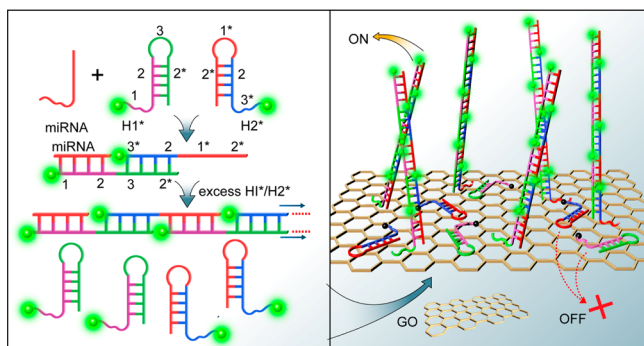
2. RESULTS AND DISCUSSION

The new strategy of the proposed HCR/GO method for miRNA detection is illustrated in Figure 1 by using let-7a as a proof-of-concept target. A pair of hairpin DNA probes each

Figure 1. Schematic illustration of the proposed HCR/GO platform for miRNA detection.

bearing a fluorophore at the sticky terminal are specifically designed according to the sequence of let-7a (denoted as H1* and H2*). In the absence of let-7a, H1* and H2* can coexist stably in solution. When let-7a is present, it hybridizes with the sticky end of H1* (1−2) and opens the hairpin through an unbiased strand-displacement interaction. The newly released sticky sequence of H1* (3−2*) will further hybridize with the sticky end of H2* (3*−2) to open its hairpin and expose a new sticky end on H2* (1*−2*). The sequence of this sticky end is identical to that of let-7a. In this manner, each miRNA molecule can specifically trigger a chain reaction of hybridization events between H1* and H2* and yield long nicked dsDNA with accumulated fluorescence signals. When GO is added into the solutions after HCR, the free H1* and H2* would be closely adsorbed onto GO surface via $\pi-\pi$ stacking.[23,24] As a result, the fluorescence can be efficiently quenched, as shown in Figure 2 (green line). As also can be
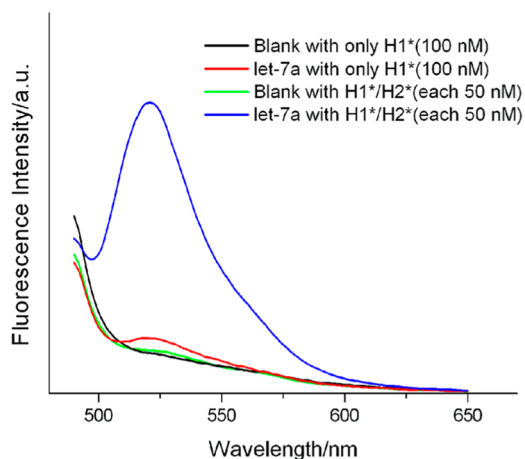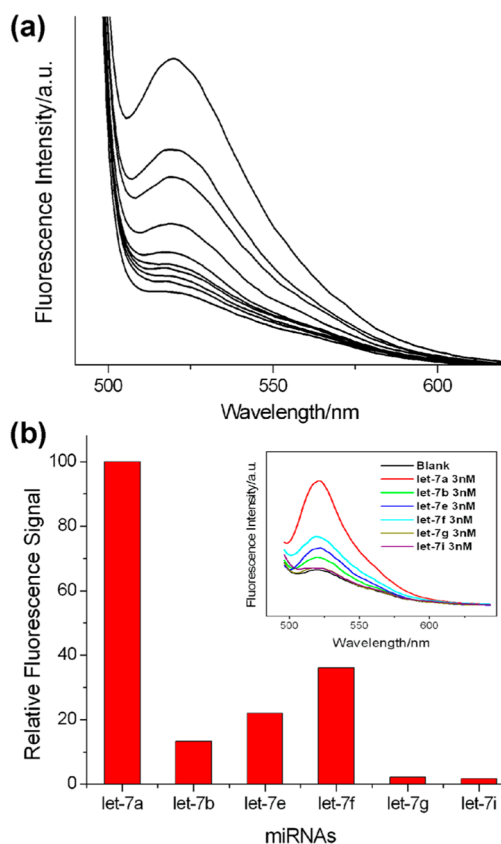

Figure 2. Fluorescence spectra of the HCR/GO platform by using H1*/H2* (50 nM each) or only H1* (100 nM) as the hairpin probes in the presence of 5 nM let-7a. Blank samples were treated as the same without adding let-7a. Other experimental conditions: GO, 25 μg/mL; λ_{EX} = 480 nm.

seen from Figure 2 (blue line) that the HCR products remain strong fluorescence signal in the presence of GO. These phenomena clearly confirm that H1* and H2* monomers can be closely adsorbed on GO surface, resulting in effective fluorescence quenching. According to the literatures,[23−27] the fluorescence quenching may be ascribed to the fluorescence resonance energy transfer (FRET) from the fluorophores to the GO. However, upon the addition of let-7a, HCR proceeds, and

the interaction between HCR products and GO will be remarkably weakened, making the fluorescence maintained. To verify that the fluorescence signal is indeed resulted from let-7a-triggered HCR but not from the one-step reaction with only H1*, an additional experiment is carried out by only using H1* as the hairpin probe. As can be seen from Figure 2 (red line), the very weak fluorescence signal of the system by using only H1* as the probe clearly indicates that the miRNA-induced fluorescence is undoubtedly resulted from HCR. Furthermore, the formation of HCR-generated long nicked dsDNA is also proved by electrophoresis analysis (see Figure S2 in the Supporting Information).

Figure 3a shows the fluorescence spectra of the HCR/GO system in the presence of different concentrations of let-7a

Figure 3. (a) Fluorescence spectra of the HCR/GO sensing platform in the presence of different concentrations of let-7a miRNA (from bottom to top: 0, 1 pM, 10 pM, 100 pM, 500 pM, 1 nM, 2 nM, 3 nM, 4 nM, 5 nM). Experimental conditions: GO, 25 μg/mL; H1*, 50 nM; H2*, 50 nM; λ_{EX} = 480 nm. (b) The specificity evaluation of the proposed HCR/GO assay. The concentrations of all the miRNAs of let-7 family are 3 nM.

under optimized conditions (see the Supporting Information). It can be seen that the fluorescence of H1* and H2* hairpin probes can be efficiently quenched by GO, and a gradual increase of the fluorescence signal is observed as the let-7a concentration increases from 1 pM to 5 nM. When the let-7a concentrations are further elevated, the fluorescence signals are almost stable and no obvious signal changes are observed in the range of 5−15 nM (data not shown). The reason may be that when the concentration of let-7a is higher than 5 nM, H1*/H2* with fixed concentrations would be exhausted and the amount of fluorophores accumulated on the HCR products are

almost the same, resulting in similar fluorescence signals after the addition of GO. Very recently, several groups have separately developed GO-based nucleic acid sensors on the basis of 1:1 binding modes, namely, one target molecule can only hybridize with one fluorescent DNA probe and recover the fluorescence of single fluorophore from the GO surface.[23−26] The detection limit of these assays for nucleic acid is generally in the range of 100 pM to 10 nM, indicating that the sensitivity of the proposed HCR/GO sensing platform is more than 2 orders of magnitude higher. Compared with these GO-based DNA assays of 1:1 binding modes, in the HCR/GO assay, one target can produce a long dsDNA with alternating H1* and H2* and therefore prevent numerous fluorophores from quenching, resulting in the greatly improved sensitivity.

Furthermore, several let-7 miRNA family members are selected to evaluate the specificity of the HCR/GO-based assay. As can be seen from Figure 3b, only let-7a induces a great fluorescence enhancement and the other let-7 miRNAs with one-base difference (let-7e, let-7f), two-base difference (let-7b, let-7g), or four-base difference (let-7i) fail to generate significant fluorescence signals. The HCR/GO assay can clearly discriminate one-base difference among the miRNA targets, indicating a high specificity.

To test whether the proposed method is generally applicable for detecting other types of nucleic acid sequences, we further apply this design to the detection of a model DNA fragment (see the Supporting Information). Similar results are obtained as those for let-7a detection. The fluorescence intensity increases gradually as the DNA concentration increases from 1 pM to 5 nM, and the fluorescence signal produced by complementary DNA target can be clearly discriminated from that of one-base mismatched, three-base mismatched, and one-base deleted DNA sequences (see Figure S6 in the Supporting Information). These results demonstrate that the proposed HCR/GO strategy may be extended for detection of various kinds of nucleic acid by accordingly designing specific H1* and H2* hairpin probes.

Figure 4 shows the representative fluorescence imaging results of the HCR/GO system under different conditions. It can be seen from Figure 4a that in the absence of GO, intense fluorescence signals can be observed in the whole field of view for the solution containing only H1*/H2* without let-7a. However, the strong fluorescence can be completely quenched when GO is added, as shown in Figure 4b. Furthermore, one can see from Figure 4b−d that bright fluorescent spots will emerge in the presence of let-7a target, and the fluorescence signals can be greatly enhanced with the increase of let-7a in the HCR/GO system. The fluorescence spectrum shown in Figure 4e indicates that the bright fluorescence areas appearing in panels c or 4d in Figure 4 undoubtedly originated from FAM fluorophores tagged on H1* and H2*.

Most interestingly, as shown in Figure 4b−d, GO can be clearly observed in the bright-field images. By comparing the bright-field images with the corresponding fluorescence images shown in c and d in Figure 4, one can see that the positions of GO and the bright fluorescence areas are completely overlapped, which can be clearly identified from the merged images. These results demonstrate that the target-induced fluorescence signals of the HCR/GO system are dominantly located on the GO surface instead of in the solution.

According to the principle of HCR, a short single-stranded sticky end will always exist at the terminal of the HCR-generated nicked dsDNA. So the HCR products should be
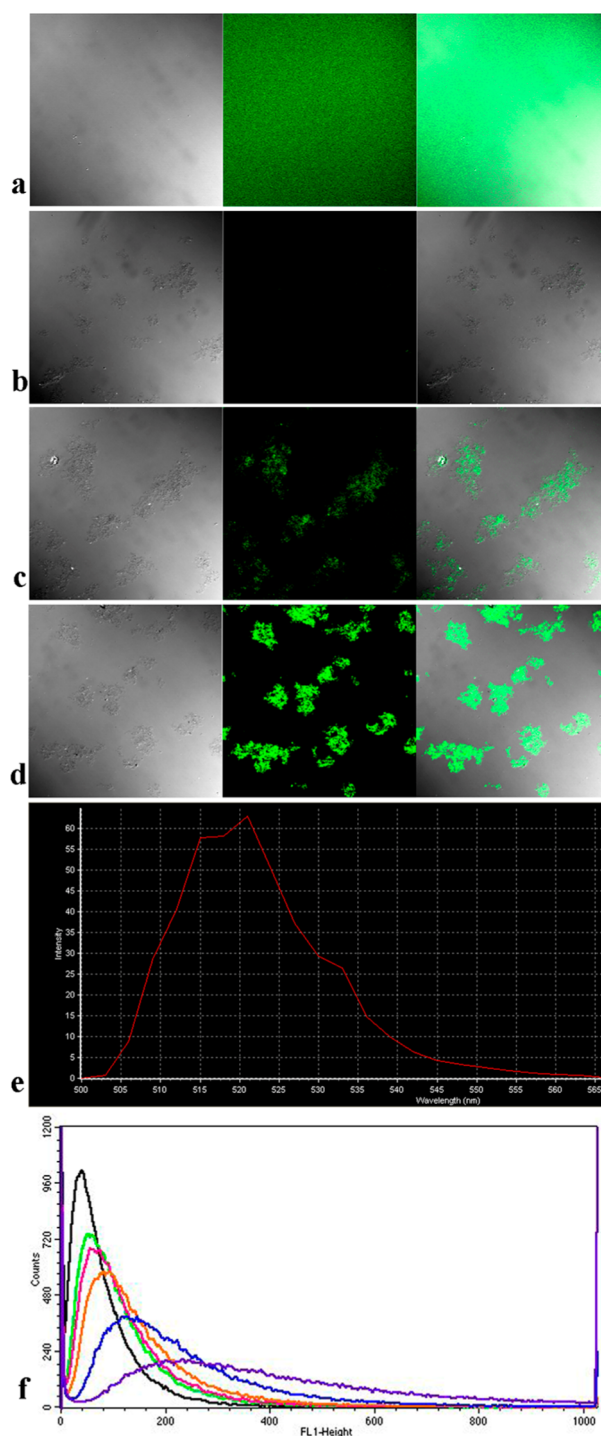
Figure 4. (a−d) Representative fluorescence images of the HCR/GO sensing platform for let-7a under different conditions: (a) only H1*/H2* without let-7a and GO; (b) H1*/H2* with GO; (c) H1*/H2* with 0.5 nM let-7a and GO; (d) H1*/H2* with 5 nM let-7a and GO; In panels a−d, the left columns represent the bright-field images, the middle columns represent the fluorescence images, and the right columns represent the merged images of the left and the middle columns; (e) typical fluorescence spectrum of the bright spots on GO surface in the fluorescence image of d; (f) typical flow cytometry graph showing the response of the HCR/GO platform to different concentrations of target (the peaks from left to right: blank, 50 pM, 100 pM, 0.5 nM, 3 nM, 5 nM). Other experimental conditions are the same as shown in Figure 3.

adsorbed on the GO surface due to the strong $\pi-\pi$ stacking effect between the sticky ends of HCR products and GO. Although the HCR products are anchored on GO surface, most of the accumulated fluorophores on the dsDNA are far away from the nearby surface of GO and maintain their fluorescence since only the sticky end of the HCR products are adsorbed on GO. Therefore, GO not only quenches the fluorescence of unreacted H1* and H2* to eliminate the background but also accumulates the target-induced fluorescence on their surface to obtain clear fluorescence images. The very interesting phenomenon is of great significance for the fluorescence imaging analysis.

Moreover, because the accumulated fluorescence signals of HCR are enriched on GO surface, it also allows the direct readout of HCR/GO system through a flow cytometer without requirement of any separation steps. As shown in the flow cytometry graph (Figure 4f), the fluorescence intensities of the GO are found to increase proportionally with the increase of target in the HCR/GO system.

3. CONCLUSION

In conclusion, a novel enzyme-free signal amplification approach for miRNA detection is developed in this work by combining the advantageous features of HCR and GO. Integrating HCR strategy for signal amplification with selective fluorescence quenching effects of GO provides a versatile sensing platform for miRNA with greatly improved sensitivity, simple operation and low cost. The sensitivity of the proposed HCR/GO system is more than 2 orders of magnitude higher compared with those of recently reported GO-based fluorescent nucleic acid assay with 1:1 binding mode. More interestingly, we demonstrate for the first time that the enriched fluorescence signals of the HCR products are dominantly gathered on the GO surface instead of in the solution, which further allows the signal readout of HCR via fluorescence microscope or flow cytometer by using GO as a robust signal-enriching matrix, showing great potential of the proposed HCR/GO platform for in situ fluorescence imaging or flow cytometry analysis of miRNA and various biomolecules.

ASSOCIATED CONTENT

Ⓢ Supporting Information

Detailed experimental procedures, optimization of the experimental conditions. This material is available free of charge via the Internet at http://pubs.acs.org.

AUTHOR INFORMATION

Corresponding Author
*E-mail: liuch@hbu.edu.cn; lzpbd@hbu.edu.cn.

Notes
The authors declare no competing financial interest.

ACKNOWLEDGMENTS

REFERENCES

(1) Bartel, D. P. *Cell* **2004**, *116*, 281−297.

(2) Farh, K. K.-H.; Grimson, A.; Jan, C.; Lewis, B. P.; Johnston, W. K.; Lim, L. P.; Burge, C. B.; Bartel, D. P. *Science* **2005**, *310*, 1817−1821.

(3) Arenz, C. *Angew. Chem., Int. Ed.* **2006**, *45*, 5048−5050.

(4) Wark, A. W.; Lee, H. J.; Corn, R. M. *Angew. Chem., Int. Ed.* **2008**, *47*, 644−652.

(5) Válóczi, A.; Hornyik, C.; Varga, N.; Burgyán, J.; Kauppinen, S.; Havelda, Z. *Nucl. Acids Res.* **2004**, *32*, e175.

(6) Lee, I.; Ajay, S. S.; Chen, H.; Maruyama, A.; Wang, N.; McInnis, M. G.; Athey, B. D. *Nucl. Acids Res.* **2008**, *36*, e27.

(7) Chen, C.; Ridzon, D. A.; Broomer, A. J.; Zhou, Z.; Lee, D. H.; Nguyen, J. T.; Barbisin, M.; Xu, N. L.; Mahuvakar, V. R.; Andersen, M. R.; Lao, K. Q.; Livak, K. J.; Guegler, K. J. *Nucl. Acids Res.* **2005**, *33*, e179.

(8) Raymond, C. K.; Roberts, B. S.; Garrett-Engele, P.; Lim, L. P.; Johnson, J. M. *RNA* **2005**, *11*, 1737−1744.

(9) Yan, J. L.; Li, Z. P.; Liu, C. H.; Cheng, Y. Q. *Chem. Commun.* **2010**, *46*, 2432−2434.

(10) Hartig, J. S.; Grüne, I.; Najafi-Shoushtari, S. H.; Famulok, M. *J. Am. Chem. Soc.* **2004**, *126*, 722−723.

(11) Allawi, H. T.; Dahlberg, J. E.; Olson, S.; Lund, E.; Ma, W. P.; Takova, T.; Neri, B. P.; Lyamichev, V. I. *RNA* **2004**, *10*, 1153−1161.

(12) Cheng, Y. Q.; Zhang, X.; Li, Z. P.; Jiao, X.; Wang, Y.; Zhang, Y. *Angew. Chem., Int. Ed.* **2009**, *48*, 3268−3272.

(13) Jia, H. X.; Li, Z. P.; Liu, C. H.; Cheng, Y. Q. *Angew. Chem., Int. Ed.* **2010**, *49*, 5498−5501.

(14) Li, C. P.; Li, Z. P.; Jia, H. X.; Yan, J. L. *Chem. Commun.* **2011**, *47*, 2595−2597.

(15) Dirks, R. M.; Pierce, N. A. *Proc. Natl. Acad. Sci. U.S.A.* **2004**, *101*, 15275−15278.

(16) Venkataraman, S.; Dirks, R. M.; Rothemund, P. W. K.; Winfree, E.; Pierce, N. A. *Nat. Nanotechnol.* **2007**, *2*, 490−494.

(17) Peng, Y.; Choi, H. M. T.; Calvert, C. R.; Pierce, N. A. *Nature* **2008**, *451*, 318−322.

(18) Wang, F.; Elbaz, J.; Orbach, R.; Magen, N.; Willner, I. *J. Am. Chem. Soc.* **2011**, *133*, 17149−17151.

(19) Wang, F.; Elbaz, J.; Willner, I. *J. Am. Chem. Soc.* **2012**, *134*, 5504−5507.

(20) Shimron, S.; Wang, F.; Orbach, R.; Willner, I. *Anal. Chem.* **2012**, *84*, 1042−1048.

(21) Huang, J.; Wu, Y.; Chen, Y.; Zhu, Z.; Yang, X.; Yang, C. J.; Wang, K.; Tan, W. *Angew. Chem., Int. Ed.* **2011**, *50*, 401−404.

(22) Choi, H. M. T.; Chang, J. Y.; Trinh, L. A.; Padilla, J. E.; Fraser, S. E.; Pierce, N. A. *Nat. Biotechnol.* **2010**, *28*, 1208−1212.

(23) Dong, H.; Gao, W.; Yan, F.; Ji, H.; Ju, H. *Anal. Chem.* **2010**, *82*, 5511−5517.

(24) Lu, C. H.; Li, J.; Liu, J. J.; Yang, H. H.; Chen, X.; Chen, G. N. *Chem.—Eur. J.* **2010**, *16*, 4889−4894.

(25) He, S.; Song, B.; Li, D.; Zhu, C.; Qi, W.; Wen, Y.; Wang, L.; Song, S.; Fang, H.; Fan, C. *Adv. Funct. Mater.* **2010**, *20*, 453−459.

(26) Lu, C. H.; Yang, H. H.; Zhu, C. L.; Chen, X.; Chen, G. N. *Angew. Chem., Int. Ed.* **2009**, *48*, 4785−4787.

(27) Zhen, S. J.; Chen, L. Q.; Xiao, S. J.; Li, Y. F.; Hu, P. P.; Zhan, L.; Peng, L.; Song, E. Q.; Huang, C. Z. *Anal. Chem.* **2010**, *82*, 8432−8437.

6453

dx.doi.org/10.1021/am302268t | *ACS Appl. Mater. Interfaces* 2012, 4, 6450−6453